

A High Capacity Li-Ion Cathode: The Fe(III/VI) Super-Iron Cathode

Stuart Licht

Department of Chemistry and Institute of Basic Energy Science and Technology, George Washington University, Washington, DC 20052, USA; E-Mail: slicht@gwu.edu; Tel.: +1-703-726-8225

Received: 31 March 2010 / Accepted: 12 April 2010 / Published: 6 May 2010

Abstract: A super-iron Li-ion cathode with a 3-fold higher reversible capacity (a storage capacity of 485 mAh/g) is presented. One of the principle constraints to vehicle electrification is that the Li-ion cathode battery chemistry is massive, and expensive. Demonstrated is a 3 electron storage lithium cathodic chemistry, and a reversible Li super-iron battery, which has a significantly higher capacity than contemporary Li-ion batteries. The super-iron Li-ion cathode consists of the hexavalent iron (Fe(VI)) salt, Na₂FeO₄, and is formed from inexpensive and clean materials. The charge storage mechanism is fundamentally different from those of traditional lithium ion intercalation cathodes. Instead, charge storage is based on multi-electron faradaic reduction, which considerably enhances the intrinsic charge storage capacity.

Keywords: cathode; Li-ion; super-iron; battery; electric vehicle; lithium battery

1. Introduction

Vehicle electrification provides significant advantages of fuel efficiency, which will decrease greenhouse gas emission, decrease the dependence on fossil fuel resources, and facilitate the transition to the renewable energy economy. However the rate of societal transition to electric vehicles is constrained by the low travel range and high battery cost of these vehicles. One of the principle constraints to vehicle electrification is that the Li-ion cathode battery chemistry is massive, and expensive. Demonstrated here is a transformative 3e- storage lithium cathodic chemistry, and a reversible Li super-iron battery with 3-fold higher capacity than contemporary cathodes. This super-iron Li-ion cathode has a storage capacity of 485 mAh/g, consists of the hexavalent iron (FeVI) salt, Na₂FeO₄, and is formed from inexpensive and clean materials. The charge storage mechanism is fundamentally different from those of traditional lithium ion intercalation cathodes.

Instead, charge storage is based on multi-electron faradaic reduction, which considerably enhances the intrinsic charge storage capacity.

The introduction of Li-ion systems has substantially increased electrochemical energy storage capacity [1]. Yet, contemporary rechargeable lithium batteries have only one fifth the volumetric energy density of gasoline, and require five times the gas tank volume to travel the same distance [2]. The cathode comprises the main mass component of contemporary Li-ion batteries. For example, the commonly used LiCoO_2 cathode and Li-Co-Mn-Ni variants have capacities of 80–150 mAh/g, but are cost limited by the relative scarcity and high price of cobalt (which is up two orders of magnitude more expensive than iron). The cobalt is associated with significant toxicity hazards.

An alternative to LiCoO_2 cathode, LiMn_2O_4 , has an even lower capacity of 100 mAh/g. A popular new cathode LiFePO_4 , contains divalent iron, Fe(II), and can store up to 170 mAh/g [3,4]. An attraction of this cathode is the availability and low cost of the source reagents (iron is the most common metal in the earth's crust). LiFePO_4 can sustain higher power densities than equivalent cobalt or manganese cathodes. However, Li-ion LiFePO_4 batteries operate at lower voltage than those with cobalt and manganese based cathodes, and also have approximately 20% lower energy storage density.

Development of 3e- Fe(VI) charge storage. An unusual class of iron salts was pioneered by our group as inorganic charge storage salts in 1999, and named super-irons due to their highly oxidized hexavalent iron state [5,6].

Key milestones in the super-iron battery development to date are of Table 1.

Table 1. Timeline of Fe(VI) charge storage development.

Year	Development	Reference
1999	introduction of super-iron charge storage & super-iron alkaline battery	[5]
2000**	introduction of super-iron lithium primary (single discharge) battery	[7]
2001	demonstration of the solid state stability of the hexavalent iron	[8]
1999-5	chemical syntheses of an array of super-iron salts	[5,7,9-16]
2000-4	inexpensive, electrochemical syntheses of super-iron salts	[17-26]
2003-5**	electrolyte optimization for super-iron lithium batteries	[27,28]
2003	reversibility of alkaline, nanothick (3 nm) Fe(VI) cathodes	[29]
2006	rechargeable alkaline super-iron battery	[30]
2006**	reversibility of non-aqueous, nanothick (3 nm) Fe(VI) cathodes	[31]
2007-8	zirconia encapsulation–stabilization of alkali super-irons	[32-35]
2009**	rechargeable super-iron lithium battery, 4 V cathode	[6]

**=lithium super-iron battery development.

2. Results and Discussion

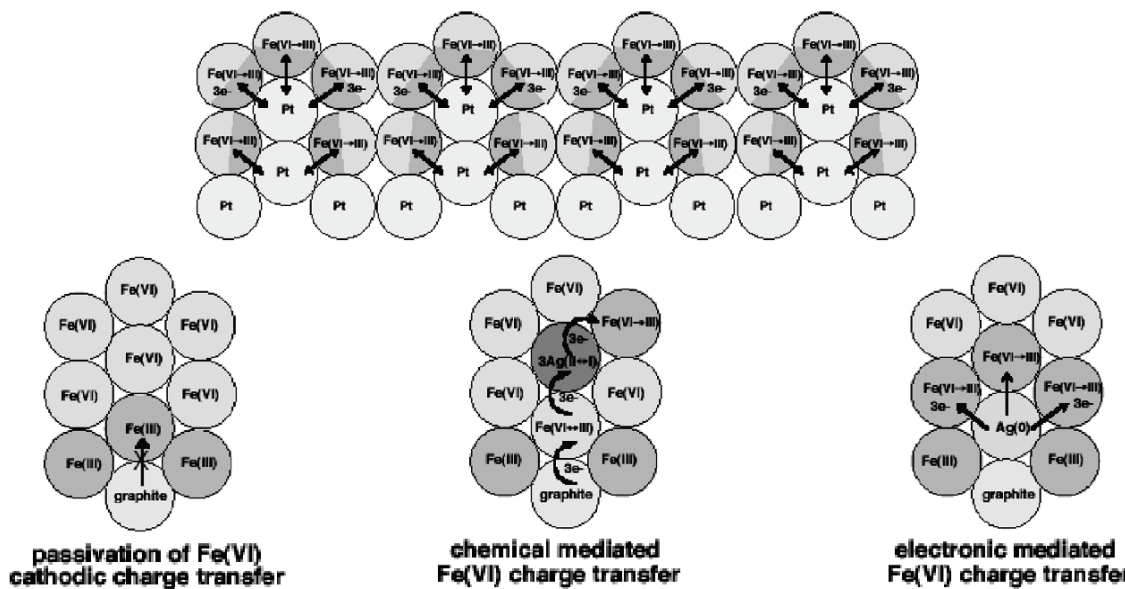
2.1. The challenge of facile Fe(VI) charge transfer

The principal limitation to facile Fe(VI) charge transfer has been passivation of the couple due to resistive buildup of low-conductivity ferric (Fe(III)) salts, as schematically represented in the lower left corner of Scheme 1 [32,36,37]. We have demonstrated that the addition of simple transition metal

oxides, such as manganese or silver oxide (shown in the scheme), to form a composite with alkali or alkali earth super-irons, considerably facilitates the rate of super-iron charge transfer through chemical and mediation of charge transport mechanisms [38-42].

Chemical mediation acts to displace passivating Fe(III) centers into the bulk and away from the current collectors, while the electronic mediation provides alternative, more conductive pathways for charge transport. We have also demonstrated that a zirconia overlayer facilitates alkal Fe(VI) charge transfer in alkali media [32-35]. Most recently, we have also shown that an external conductive matrix, such as platinized, platinum considerably enhances reversible, non-aqueous Fe(VI) charge transfer [5].

Scheme 1. Modes of Fe(VI) charge transfer and passivation. Bottom: middle-Chemical mediated, and right-electronic mediated, Fe(VI) charge transfer. Bottom-left: Fe(III) inhibition and passivation of charge transfer. Top: Nanofilm enhanced reversible Fe(VI) charge transfer.



2.2. Reversible non-aqueous 3e- Fe(VI) charge storage

The basis for improved electrochemical storage capacity using the super-iron Li battery:

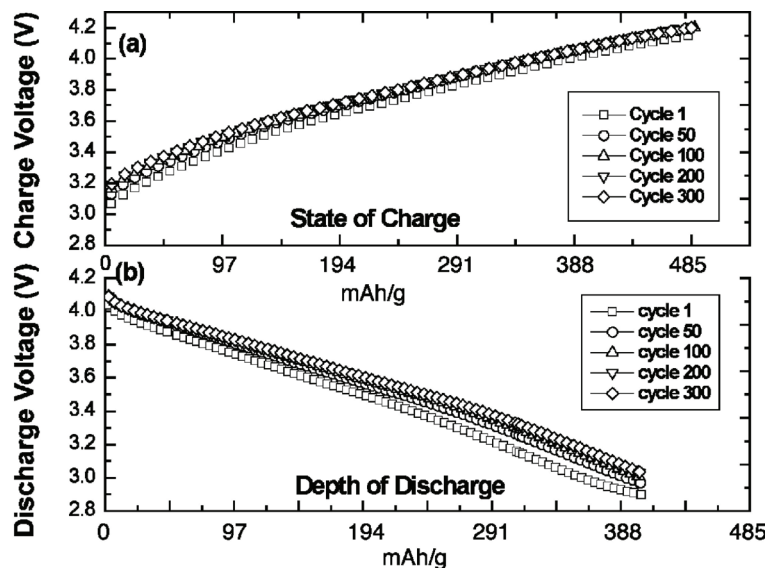
- Fe(VI) nonaqueous charge transfer is constrained by reduction, not intercalation.
- Fe(VI) cathodes store the charge equivalent to 3 electrons per iron center,
- an extended conductive matrix facilitates reversible Fe(VI) reduction,
- the redox Fe(VI) potential is 0.25 V larger than that of Li-Mn or Li-Co cathodes.

The Fe(VI) redox storage potential *versus* lithium has increased from an observed 3 V, to over 4 V, in the past 3 years. With advent of the 485 mAh/g lithium non-aqueous cathode, and with use of the conductive matrix, the reversible, non-aqueous super-iron has increased 200 fold in thickness (from 3 nm to over 600 nm).

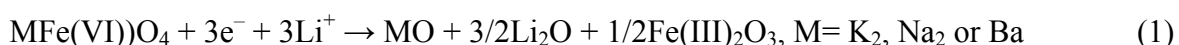
In 2009, we presented the first reversible super-iron Li batteries, cells operating at high voltage (over 4 volt) and a cathode capacity of 485 mAh/g, several fold higher than the cathodes in contemporary Li-ion batteries [6]. The capacity is based on the intrinsic three electron storage of

Na_2FeO_4 , 50 nm thick cathodes were cycled at over 90% DOD (depth of discharge), and 191 and 573 nm thick cathodes were cycled at over 80% (400 mAh/g). Charge and discharge voltage during 300 recharge cycles are shown in Figure 1.

Figure 1. Extended galvanostatic cycling charge-transfer behavior for a super-iron Li battery containing a 191-nm thick Fe(III/VI) Na_2FeO_4 cathode film. (a) Cell potential during charge and (b) cell potential during discharge. Charge/discharge cycle numbers are indicated. Results are detailed in Licht, Wang, Gourdin, Enhancement of Reversible Nonaqueous Fe(III/VI) Cathodic Charge Transfer, *Journal of Physical Chemistry, C*, 133, 9884–9891 (2009).



Rather than the typical intercalation mechanism of conventional Li and Li-ion cathodes, the super-iron discharge involves reduction from Fe(VI to III), as confirmed by AA, Mossbauer and charge measurements in the electrochemical processes. To date this was demonstrated as 3 Faraday per mole of Na_2FeO_4 (an intrinsic 485 mAh/g capacity), K_2FeO_4 (an intrinsic 408 mAh/g capacity) or BaFeO_4 (314 mAh/g) in accord with the discharge mechanism [6]:



2.3. Preparation of Super-Iron Cathode Films

The electrochemical preparation of Fe(III/VI) super-iron thin films cathodes on an extended conductive matrix significantly facilitates such film's nonaqueous, reversible charge transfer. Fe(VI) salts can exhibit higher cathodic capacity and environmental advantages, and the films are of relevance toward the next generation charge storage chemistry for reversible cathodes. These films were electrochemically deposited by electrochemical reduction of Na_2FeO_4 , which retains an intrinsic 3 e^- cathodic charge storage capacity of 485 mAh g⁻¹. The influence on cathode reversibility, capacity and charge retention was probed as function of film deposition conditions (including the deposition potential and stirring rate, and the concentration of NaOH and K_2FeO_4 , in the deposition electrolyte).

Initially to optimize deposition conditions, super-iron films were electrodeposited from various alkaline $K_2FeO_4/NaOH$ solutions at an applied potentiostatic voltage of 0.11 V vs. Ag/AgCl in a voltammetric Plexiglas cell, and optimized as a function of solution composition. Subsequently, super-iron films were consistently electrodeposited from 50 mM K_2FeO_4 dissolved in stirred (magnetic bar), 8.0 M NaOH in a voltammetric Plexiglas cell at a galvanostatic current of 10.0 mA. The working electrode was a 1 cm² platinum disc or a 1 cm² platinized, platinum disc. The auxiliary electrode was a platinum rod, and the reference electrode was an Ag/AgCl/ KCl (sat) encased in a 0.1 M $NaNO_3$ jacket. Solutions were initially de-aerated with nitrogen gas for a minimum of 5 min prior to the electro-deposition. A N₂ gas atmosphere was maintained over the solution during the electrodeposition. The film electrode was carefully rinsed with 8.0 M NaOH solution, air dried for 30 minutes, and then vacuum dried for 2 days prior to use.

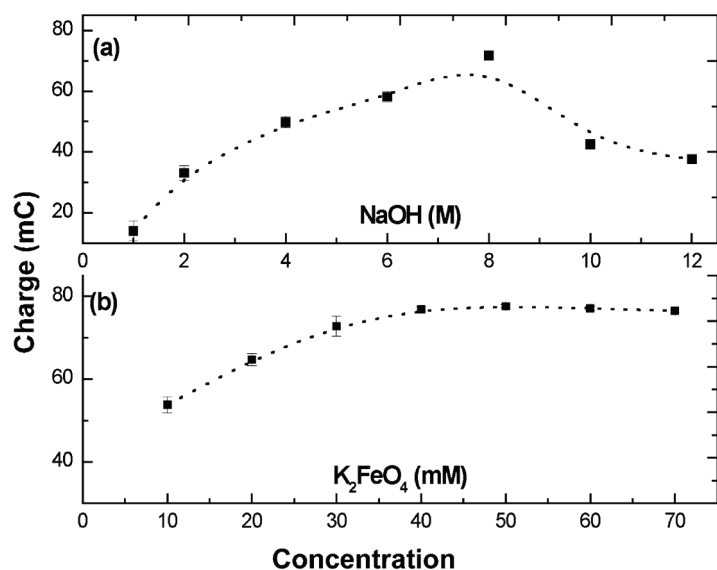
During the optimization of the electrodeposition process, the surface of the working electrode was rinsed at each end of the experiment by an oxidative linear potential scan in 1.0 M HCl solution. Employed voltammetric Plexiglas cells were consistently, cleaned by soaking overnight in a solution of 10⁻² M nitric acid, followed by DI water rinse, and results presented are the average of three replicate measurements. For Fe(III/VI) film formation, at the optimized deposition potential employed, the electrodeposition via the 3 electron reduction of Fe(VI) to Fe(III) substantially dominates, permitting the current efficiency to be assumed as 100%. Hence, the intrinsic capacity of the super-iron films determined by integrating the current-time response curve, Q (C = coulombs = ampere seconds), provides a quantitative measure of the intrinsic charge capacity of the super-iron films and, for convenience, a relative (not absolute) measure of the film thickness. The relative comparison of film thicknesses, T , is quantitative for all compared electrodes. For example a 19 nm Fe(III/VI) films contains 69 nanaomole of Fe per cm², and is capable of storing 20 mC of intrinsic capacity per cm² (based on the observed 3 electrons of storage per Fe(III/VI) center). Similarly, thicker deposited 57, 191 and 573 nm Fe(III/VI) films used in this study, have an intrinsic storage capacity respectively of 60, 202 and 605 mC per cm².

The solid state stability (stable to > 99.9% year retention of the Fe(VI) valence state), and storage time, for K_2FeO_4 is much greater than for Na_2FeO_4 , and hence it has been our chemical dissolution salt of choice. In this study, the effects on Fe(III/VI) charge storage on smooth platinum were conducted by varying the concentrations of $[K_2FeO_4]$, $[NaOH]$, electrodeposition potential and magnetic stirring rate, respectively.

Figure 2a presents the effect of the electrolyte, NaOH, concentration on charge storage in 50 mM K_2FeO_4 . It is seen that the Fe(III/VI) charge storage capacity increased with increasing the concentration of NaOH from 1.0 to 8.0 M, while an increase beyond 8.0 M NaOH led to a decrease of Fe(III/VI) charge storage. Increasing NaOH concentration (from 1.0 to 8.0 M) will inhibit the K_2FeO_4 solution phase decomposition process (Equation 7), stabilizing the $MFeO_4^-$ or FeO_4^{2-} species (Equations 12 and 13), and as a result, the Fe(III/VI) charge storage is increased. In competition with this is the decrease in equivalent ionic conductivity of hydroxide with increasing concentration. For the NaOH electrolyte, this decrease is significant. For example at 18°C the equivalent conduction of NOH solutions, decrease from 160 to 108 S cm²/equivalent, as concentration increases from 1 to 3 M, and the decrease is precipitous in more concentrated NaOH (decreasing to 69 S cm²/ equivalent in 5 M NaOH). Consistent with the observed decrease in charge storage at 8 M NaOH, this decrease in

mobility at higher concentrations appears to dominate over the stabilization enhancement. Therefore, in order to obtain a favorable charge storage, a compromise between decomposition and ion mobility needs to be considered. Figure 2b presents the concentration effect of K_2FeO_4 on charge storage in 8.0 M NaOH. It was found that the storage charge increased with increasing the concentration of K_2FeO_4 until a plateau was formed about 45 mM of K_2FeO_4 , which approaches the saturation point of K_2FeO_4 in 8.0 M NaOH. In subsequent experiments in this study, 8.0 M of NaOH and 50.0 mM of K_2FeO_4 were used in the following experiments, except in noted special cases. In this concentrated alkaline environment diffusion processes should be facilitated. Hence, variation of the (magnet bar) stirring rate was also probed, and generally, the higher the stirring rate, the greater the charge storage which can be obtained in the deposited Fe(III/VI) films; this is consistent with the expected compression of the diffusion layer with an increase in solution turbulence.

Figure 2. Electrodeposition optimization of a Fe(III/VI) film. Deposition conditions—applied potential: 110 mV *versus* Ag/AgCl; deposition time 10 s on a smooth platinum electrode; stirring rate: maximum, without disruptive turbulence: (a) the effect of NaOH concentration on charge storage in 50 mM K_2FeO_4 and (b), the effect of K_2FeO_4 concentration on charge storage in 8.0 M NaOH.



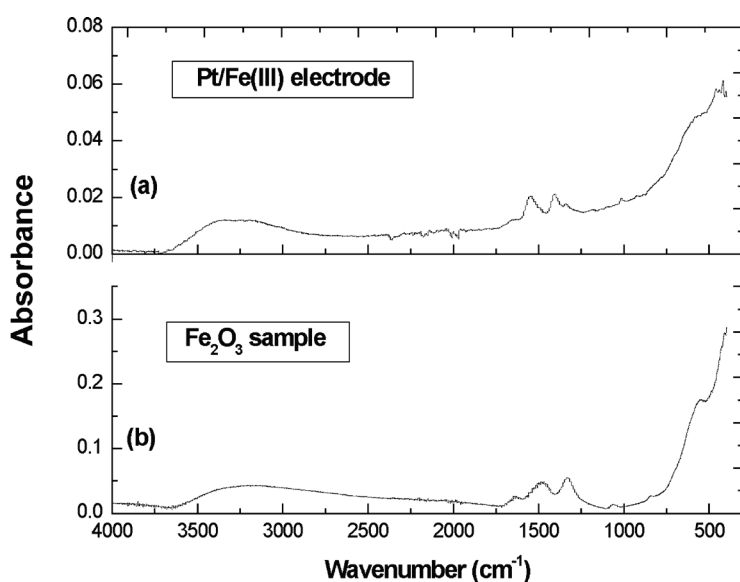
2.4. Characterization of Super-Iron Cathode Films

The 3-electron reduction of Fe(VI) can produce a variety of Fe(III) oxide and oxyhydroxide species such as (α, γ Fe_2O_3) and ($\alpha, \gamma, \beta, \delta$ FeOOH). Sodium, over potassium, species will dominate in the 8 M N^+ , 0.01 M K^+ deposition solution, and a variety of cation-containing ferric salts such NaFeO_2 are also possible in the film. Well-defined Fe_2O_3 particles gave three fundamental bands ranged from 500 cm^{-1} , 400 cm^{-1} to 300 cm^{-1} respectively, and the bands shifted with varying in size, shape, internal structure and aggregation of particles. In our experiment, the surface morphologies of thin Fe(III) film on smooth platinum were examined by a Nicolet Nexus 670 Fourier Transform Infrared Spectrophotometer.

Figure 3a presents the FTIR diffuse reflectance spectra (in absorbance mode) of a 191 nm thin Fe(III) film which was freshly electrodeposited on a 1 cm^2 platinum disk. A single peak at $\sim 429 \text{ cm}^{-1}$,

and a shoulder near 538 cm^{-1} are observed (far infrared spectra less than 400 cm^{-1} was not examined due to the instrumental limitations). For comparison, nanocrystalline $\gamma\text{-Fe}_2\text{O}_3$ particles were synthesized, and the FTIR absorption spectra of this particle is showed in Figure 3b. Two adjacent peaks near 1500 cm^{-1} appear to be associated with residual free hydroxide. The strong similarity between our Fe(VI) electrodeposited film Fe(III) and the nanocrystalline $\gamma\text{-Fe}_2\text{O}_3$ particles indicates this as a principal component of the Fe(III) film. In ongoing investigations, we continue to probe the identity of the Fe(III) centers in the reduced form of the film Fe(III/VI) films.

Figure 3. FTIR diffuse reflectance spectrum (in absorbance mode) of (a) a Pt/Fe(III) electrode and (b) a Fe_2O_3 sample. The electrodeposition conditions of Pt/Fe(III) are the same as above with $50\text{ mM K}_2\text{FeO}_4$ in 8.0 M NaOH . The Fe_2O_3 samples are freshly synthesized.

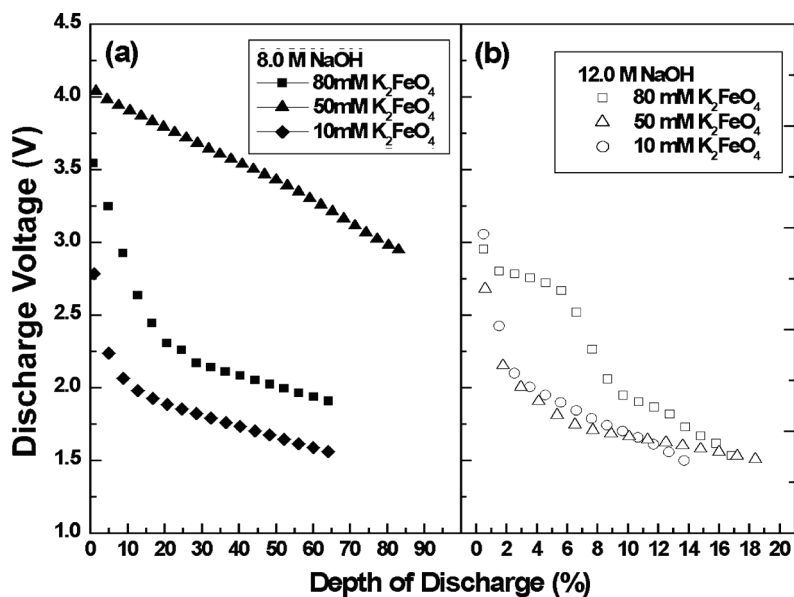


The Fe(III/VI) films were placed in a lithium cell with 1M LiPF_6 in PC: DME (1:1) electrolyte, and their quasi-reversibility characterized as a function of hydroxide and Fe(VI) concentrations in the deposition solution. Specifically, a 191 nm Fe(III/VI) on smooth platinum was galvanostatically deposited (at 10 mA , for 10s) in either 10 , 50 or $80\text{ mM K}_2\text{FeO}_4$. The film was placed in a lithium cell with 1M LiPF_6 in PC: DME (1:1) electrolyte, and cycled through periodic, galvanostatic charge/discharge cycles. Specifically, each cell was repeatedly subject to a 0.02 mA cm^{-2} charge, followed by a deep 0.01 mA cm^{-2} discharge.

Figure 4 presents the discharge voltage during the 20th discharge cycle as a function of the intrinsic, (100 mC , 3 electron) depth of discharge of these films. Figure 4a,b, respectively presents discharge cycle behavior for films prepared from either 8.0 M (4a) or 12.0 M (4b) deposition solutions. It is evident in Figure 4 that the average discharge voltage, and the depth of discharge are significantly higher for films deposited in 8 M , rather than 12 M , NaOH . Furthermore, in the preferred 8 M NaOH deposition solution, the average discharge voltage, and the depth of discharge are significantly higher for films deposited from 50 mM , rather than 10 or $80\text{ mM K}_2\text{FeO}_4$ solutions. It is evident that the charge storage and transfer behavior of Fe(III/VI) thin-film cells are significantly influenced by the electrochemical deposition conditions. In the $50.0\text{ mM K}_2\text{FeO}_4$, 8.0 M of NaOH prepared film,

the 20th discharge cycle commenced at 4.1 V and decayed to 3.1 V through an 80% depth of discharge, and no sharp decline of potential was observed within 20 cycles.

Figure 4. The discharge behavior of a 191 nm Fe(VI) film on a Pt electrode with various deposition conditions at 20th cycle. Films are deposited at a constant current of 10 mA for 10 s from electrolytes containing various $[K_2FeO_4]$ in 8.0 M (a) or 12.0 M NaOH (b). Subsequent nonaqueous galvanostatic cycling consists of charge at 0.02 mA cm^{-2} to 100% of the intrinsic $3e^-$ Fe capacity, as limited by a maximum cutOff voltage of 4.2 V, followed by discharge at 0.01 mA cm^{-2} to 90% DOD of this capacity as limited by a 1.5 V minimum voltage cutoff.



FTIR provides not only a specific "fingerprint" distinguishing the various Fe(VI) oxides, as shown in Figure 5, but importantly we have also developed it as a quantitative technique to determine the Fe(VI) salt purity through the addition of a standardized $BaSO_4$ salt [8]. Discharge of cathode replaced, commercial alkaline button cells provides rapid screening of the redox activity of alternative salts [6,10,11,14,15,19,27-35].

X-ray powder diffraction and Mössbauer are used to distinguish the variation of crystal structure and definitive nature of the iron state of super-iron oxides as a function of the state of charge/discharge of the cycled new cathode salts. As seen in Figure 6, we used these techniques to probe alkali and alkali earth super-iron oxides, and x-ray characterization of these salts has provided specific lattice parameters of their orthorhombic β - K_2SO_4 analogue structure.

As seen in Figures 1 and 6(right), we have the fascinating case of a cathode which can be reversibly, reformed by faradaic charge transfer, as in aqueous cells, but with the high voltage advantage of the nonaqueous environment.

Figure 5. IR absorption of solid K_2FeO_4 , Rb_2FeO_4 , Cs_2FeO_4 , BaFeO_4 , and SrFeO_4 , mixed with a BaSO_4 standard. From Licht, S.; Naschitz, V.; Rozen, D.; Halperin, N. Cathodic charge transfer and analysis of Cs_2FeO_4 , K_2FeO_4 and mixed alkali Fe(VI), ferrate, super-irons. *J. Electrochem. Soc.* **2004**, *151*, A1147–A1151.

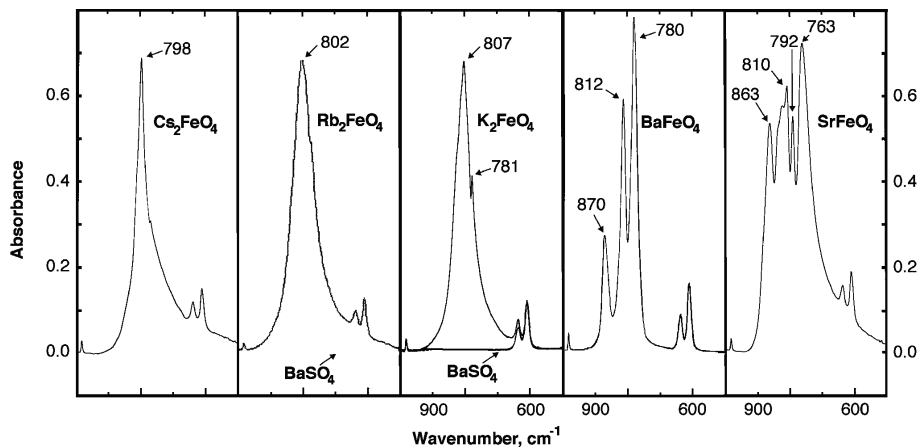
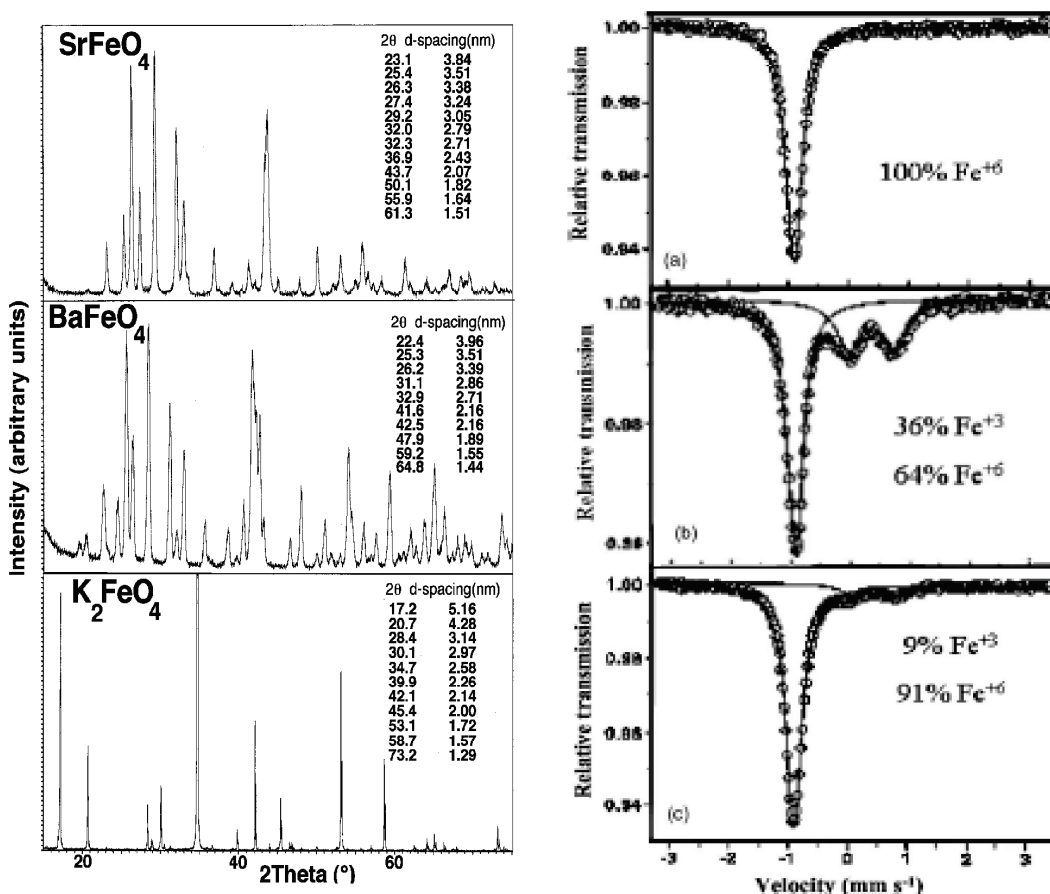


Figure 6. Left: X-ray analysis of Fe(VI) compounds, evidence of their orthorhombic β - K_2SO_4 analogue structure, from "Recent advances in the synthesis and analysis of Fe(VI) cathodes." Licht, et al., *J. Solid State Electrochem.* **2008**, *12*, 1523. Right: Mössbauer spectra of K_2FeO_4 : (a) pristine electrode, (b) polarized to 1.5V vs. Li/Li^+ , and (c) after one complete lithiation cycle. From "Study of Various ("super iron") MeFeO_4 compounds in Li salt solutions as cathode materials for Li batteries." *J. Electrochem Soc.* **2006**, *153*, A32.



3. Conclusions

Vehicle electrification provides significant advantages of fuel efficiency, which will decrease greenhouse gas emission, decrease the dependence on fossil fuel resources, and facilitate the transition to the renewable energy economy. Principle constraints to vehicle electrification include that the Li-ion cathode battery chemistry is massive and costly. Limited battery capacity (vehicle range) and cost are hurdles to implementation. This is exemplified in a recent evaluation of Li-ion batteries for use in electrified vehicles, which concludes that after yield economies of scale, the “most significant cost component at the cell-level is the cathode active material”, and which is three times more expensive than the anode material [43].

The super-iron cathode addresses the cathode challenge with a transformative $3e^-$ Fe(VI) storage Li-ion chemistry, with a capacity several fold higher than observed in conventional lithium-ion cathodes. Continued research will further advance these systems. For example, new nm-architectures need to be explored which preserve the high recharge voltage efficiency observed for the thin layer Fe(III/VI) films. As super-iron films are increased in thickness by a factor of two orders of magnitude, from a thickness of several nm [29] to a thickness approaching 1 μm [6], impedance losses increase, and impair the recharge voltage of efficiency. The thicker films retain a high coulombic efficiency, but exhibit a charge/discharge potential variation similar to super-capacitor, rather than battery, behavior. The super-iron lithium-ion battery is a Li-ion chemistry in which the cathode does not weigh down the battery, with a *transformative potential in terms of range increase of electric vehicles*.

Acknowledgements

S. Licht is grateful to the US Department of Energy and the George Washington University Institute of Basic Energy Science and Technology for partial support of this research. Yufei Wang, Gerald Gourdin and Lan Yang participated in the results reported in Figure 1 and Reference 6.

References and Notes

1. *Advances in Lithium-ion Batteries*; van Schalkwijk, W.A., Scrosati, B., Eds.; Springer: Berlin, Germany, 2002.
2. Licht, S.; Wu, H.; Yu, X.; Wang, Y. Renewable highest capacity VB_2/air energy storage. *Chem. Comm.* **2008**, *28*, 3257–3259.
3. Li, Z.; Zhang, D.; Yang, F. Developments of lithium-ion batteries & challenges of LiFePO_4 as one promising cathode material. *J. Mater. Sci.*, **2009**, *44*, 2435–2443.
4. Padhi, A.K.; Nanjundaswamy, K.S.; Goodenough, J.B. Phospho-olivines as positive-electrode materials for rechargeable lithium-ion batteries. *J. Electrochem. Soc.* **1997**, *144*, 1188–1194.
5. Licht, S.; Wang, B.; Ghosh, S. Energetic iron (VI) chemistry: The super-iron battery. *Science* **1999**, *285*, 1039–1042.
6. Licht, S.; Wang, Y.; Gourdin, G. Enhancement of reversible nonaqueous Fe(III/VI) cathodic charge transfer. *J. Phys. Chem. C* **2009**, *113*, 9884–9891.
7. Licht, S.; Wang, B. Non aqueous Iron(VI) chemistry: The lithium super-iron battery. *Electrochim. Solid State Lett.* **2000**, *3*, A 209–A212.

8. Licht, S.; Naschitz, V.; Halperin, L.; Halperin, L.; Lin, L.; Chen, J.; Ghosh, S.; Lui, B. Analysis of Ferrate(VI) compounds & super-Iron battery cathodes, FTIR, XRD, UV/Vis, ICP, electrochemical & chemical characterization. *J. Power Sources*, **2001**, *99*, 7–14.
9. Licht, S.; Wang, B.; Ghosh, S.; Jun, Li; Naschitz, V. Insoluble Fe(VI) compounds: Effects on the super-iron battery. *Electrochem. Comm.* **1999**, *1*, 522–526.
10. Licht, S.; Naschitz, V.; Ghosh, S.; Liu, B.; Halperin, N.; Halperin, L.; Rozen, D. Chemical synthesis of battery grade super-iron barium and potassium Fe(VI) ferrate compounds. *J. Power Sources* **2001**, *99*, 7–14.
11. Licht, S.; Naschitz, V.; Ghosh, S.; Lin, L.; Lui, B. SrFeO₄: synthesis, Fe(VI) characterization and the strontium super-iron battery. *Electrochem. Comm.* **2001**, *3*, 340–345.
12. Yang, W.; Wang, J.; Pan, T.; Xu, J.; Xhang, J.; Cao, C. Studies on electrochem. characteristics of K₂Sr(FeO₄)₂ electrode. *Electrochem. Comm.* **2002**, *4*, 710–715.
13. Licht, S.; Naschitz, V.; Wang, B. Rapid chemical synthesis of barium ferrate, BaFe(VI)O₄. *J. Power Sources* **2002**, *109*, 67–70.
14. Licht, S.; Naschitz, V.; Rozen, D.; Halperin, N. Cathodic charge transfer and analysis of Cs₂FeO₄, K₂FeO₄ and mixed alkali Fe(VI), ferrate, super-irons. *J. Electrochem. Soc.* **2004**, *151*, A1147–A1151.
15. Licht, S.; Yang, L.; Wang, B. Synthesis and analysis of Ag₂FeO₄ Fe(VI) ferrate super-iron cathodes. *Electrochem. Comm.* **2005**, *7*, 931–936.
16. Xu, Z.; Wang, J.; Shao, H.; Tang, Z.; Zhang, J. Preliminary investigation on the physiochemical properties of calcium ferrate. *Electrochem. Comm.* **2007**, *9*, 371–377.
17. Licht, S. Electrolytic production of solid Fe(VI) salts, PCT application No. LI00588. Patent No. WO0,121,856, 2000.
18. Lapique, F.; Valentin, G. Direct electrochemical preparation of solid potassium ferrate. *Electrochem. Comm.* **2002**, *4*, 764–766.
19. Licht, S.; Tel-Vered, R.; Halperin, L. Direct electrochemical preparation of solid Fe(VI) compounds and super-iron battery compounds. *Electrochem. Comm.* **2002**, *4*, 933–937.
20. Lee, J.; Tryk, D.; Fujishima, A.; Park, S. Electrochemical generation of ferrate in acidic media at boron-doped diamond electrodes. *Chem. Comm.* **2002**, *5*, 486–487.
21. De Koninck, M.; Brousse, T.; Belanger, D. The electrochemical generation of ferrate at pressed iron powder electrode: Effect of different parameters. *Electrochim. Acta* **2003**, *48*, 1425–1433.
22. Licht, S.; Tel-Vered, R.; Halperin, L. Towards efficient electrochemical synthesis of Fe(VI) ferrate, and super-iron battery compounds. *J. Electrochem. Soc.* **2004**, *151*, A31–A39.
23. Zhang, F.C.; Liu, Z.; Wu, F.; Lin, L.; Qi, F. Electrochemical generation of ferrate on SnO₂-Sb₂O₃/Ti electrodes in strong concentration basic condition. *Electrochem. Comm.* **2005**, *6*, 1104–1109.
24. Cañizares, P.; Arcís, M.; Sáez, C.; Rodrigo, M.A. Electrochemical synthesis of ferrate using boron doped diamond anodes. *Electrochem. Comm.* **2007**, *9*, 2286–2290.
25. Xu, Z.; Wang, J.; Mao, W.; He, W.; Chen, Q.; Zhang, J. The effects of ultrasound on the direct electrosynthesis of solid K₂FeO₄ and the anodic behaviors of Fe in 14 M KOH solution. *J. Solid State Electrochem* **2008**, *11*, 413–420.

26. Yu, X.; Licht, S. Advances in electrochemical Fe(VI) synthesis and analysis. *J. Appl. Electrochem.* **2008**, *38*, 731–742.
27. Licht, S.; Rozen, D.; Tel-Vered, R.; Halperin, L. Enhancement of nonaqueous Fe(VI) super-iron primary cathodic charge transfer. *J. Electrochem. Soc.* **2003**, *150*, A1671–A1675.
28. Koltypin, M.; Licht, S.; Tel-Vered, R.; Naschitz, V.; Aurbach, D. The Study of Licht, S.: Various ("super iron") MeFeO_4 (F^{6+} -super iron) compounds in Li salt solutions. *J. Power Sources* **2005**, *146*, 723–726.
29. Licht, S.; Tel-Vered, R. Rechargeable Fe(III/VI) super-iron cathodes. *Chem. Comm.* **2004**, *6*, 628–629.
30. Licht, S.; DeAlwis, C. Conductive matrix mediated charge transfer in Fe(III/VI): Three electron storage, reversible super-iron thin film cathodes. *J. Phys. Chem. B* **2006**, *110*, 12394–123404.
31. Koltypin, M.; Licht, S.; Nowik, I.; Levi, E.; Gofer, Y.; Aurbach, D. The study of various ("super-iron") MeFeO_4 compounds in Li salt solutions as potential cathode materials for Li batteries. *J. Electrochem. Soc.* **2006**, *153*, A32–A41.
32. Licht, S.; Yu, X.; Dhong, Z. Cathodic chemistry of high performance Zr coated alkaline materials. *Chem. Comm.* **2006**, *2006*, 4341–4343.
33. Licht, S.; Yu, X.; Qu, D. A novel alkaline redox couple: Chemistry of the $\text{Fe}^{6+}/\text{B}^{2-}$ super-iron boride battery. *Chem. Comm.* **2007**, *2007*, 2753–2755.
34. Licht, S.; Yu, X.; Wang, Y.; Stabilized alkaline Fe(VI) charge transfer: Zirconia coating stabilized super-iron alkaline batteries. *J. Electrochem. Soc.* **2008**, *155*, A1–A7.
35. Licht, S.; Yu, X.; Wang, Y.; Wu, H.; The super-iron boride battery. *J. Electrochem. Soc.* **2008**, *155*, A297–A303.
36. Ghosh, S.; Wen, W.; Urian, R.C.; Heath, C.; Srinivasamurthi, V.; Reiff, W.M.; Mukerjee, S.; Naschitz, V.; Licht, S. The reversible behavior of K_2FeO_4 . *Electrochem. Solid State Lett.* **2003**, *6*, A260–A264.
37. Yu, X.; Licht, S. Recent advances in synthesis and analysis of Fe(VI) cathodes: solution phase and solid-state Fe(VI) syntheses, reversible thin-film Fe(VI) synthesis, coating-stabilized Fe(VI) synthesis. *J. Solid State Electrochem.* **2008**, *12*, 1523–1540.
38. Licht, S.; Ghosh, S.; Naschitz, V.; Halperin, N.; Halperin, L. Fe(VI) catalyzed manganese redox chemistry: Permanganate and super-iron batteries. *J. Phys. Chem. B* **2001**, *105*, 11933–11936.
39. Licht, S.; Naschitz, V.; Ghosh, S. Silver mediation of Fe(VI) charge transfer: Activation of the K_2FeO_4 super-iron cathode. *J. Phys. Chem. B* **2002**, *106*, 5947–5955.
40. Yu, X.; Licht, S. Advances in Fe(VI) charge storage: Part II. Reversible alkaline super-iron batteries and nonaqueous super-iron batteries. *J. Power Sources* **2007**, *171*, 1010–1022.
41. Licht, S.; Ghosh, S. High power $\text{BaFe(VI)}\text{O}_4/\text{MnO}_2$ composite cathode alkaline super-iron batteries. *J. Power Sources* **2002**, *109*, 465–468.
42. Licht, S.; Naschitz, V.; Ghosh, S. Hydroxide activated AgMnO_4 alkaline cathodes, alone, and in combination with Fe(VI) super-iron, BaFeO_4 . *Electrochem. Solid State Lett.* **2001**, *4*, A209–A212.

43. Anderson, D.L. *An evaluation of current and future costs for lithium-ion batteries for use in electrified vehicle powertrains*. Master Thesis, Duke University, Durham, NC, USA, May 2009. Available online: <http://dukespace.lib.duke.edu/dspace/bitstream/10161/1007/1/Li-Ion%20Battery%20Costs%20-%20Anderson%20-%20MP%20Final.pdf> (accessed on 25 April 2010).

© 2010 by the authors; licensee MDPI, Basel, Switzerland. This article is an open-access article distributed under the terms and conditions of the Creative Commons Attribution license (<http://creativecommons.org/licenses/by/3.0/>).